PHYSICAL REVIEW D **96,** 046015 (2017)

Hyperscaling violating black hole solutions and magneto-thermoelectric DC conductivities in holography

Xian-Hui Ge

Department of Physics, Shanghai University, Shanghai 200444, People's Republic of China and Department of Physics, University of California at San Diego, San Diego, California 92037, USA

Yu Tian

School of Physics, University of Chinese Academy of Sciences, Beijing 100049, People's Republic of China

Shang-Yu Wu

Department of Electrophysics, National Chiao Tung University, Hsinchu 300, Taiwan, Republic of China

Shao-Feng Wu

Department of Physics, Shanghai University, Shanghai 200444, China and Shanghai Key Lab for Astrophysics, 100 Guilin Road, 200234 Shanghai, People's Republic of China

(Received 24 June 2016; revised manuscript received 8 November 2016; published 28 August 2017)

We derive new black hole solutions in Einstein-Maxwell-axion-dilaton theory with a hyperscaling violation exponent. We then examine the corresponding anomalous transport exhibited by cuprate strange metals in the normal phase of high-temperature superconductors via gauge-gravity duality. Linear-temperature-dependence resistivity and quadratic-temperature-dependence inverse Hall angle can be achieved. In the high-temperature regime, the heat conductivity and Hall Lorenz ratio are proportional to the temperature. The Nernst signal first increases as temperature goes up, but it then decreases with increasing temperature in the high-temperature regime.

DOI: 10.1103/PhysRevD.96.046015

I. INTRODUCTION

The surprising transport behavior of cuprate strange metal has been the subject of intense scrutiny [1]. The normal state transport of high-temperature superconductors is highly anomalous and remains one of the most challenging topics in modern condensed matter physics. The drawbacks of the conventional methods is that, based on the perturbation theory, it is hard to deal with strongly coupled many-body problems. The ubiquitous T-linear resistivity, the strong T^2 dependence of the Hall angle ϑ_H, the temperature scaling of magnetoresistance, and thermopower are some of the striking anomalies that have puzzled the physics community over the past three decades.

For decades, researchers have expended theoretical efforts on determining the relationship between the anomalous transport scaling and the quantum criticality [2–7]. Recently, the gauge-gravity duality, as a nonperturbative tool, was suggested to study the Hall angle and dc conductivity in strongly interacting critical theories [8–12]. Analytic expressions were obtained for thermo-electric conductivity tensors with a magnetic field and disorder [13–17], and it was determined that the Hall angle generically displays a different temperature dependence of resistivity [8]. This is in agreement with the two-relaxation-times model suggested by Anderson *et al.* [18,19]. Intensive studies have been conducted for obtaining numerical and analytical expressions for the transport properties of holographic theories with the translational invariance broken [20–35]. In [36,37], a scaling hypothesis was proposed to explain the unusual scaling laws for the thermopower, magnetoresistivity, and Hall Lorenz ratio. Unfortunately, this hypothesis failed in reproducing the temperature dependence of thermodynamic quantities such as specific heat and entropy density of cuprates. An alternative scaling approach was later proposed for constructing viable phenomenologies of the cuprate strange metal in [38,39]. A more convincing comparison with experimental phenomenologies is still lacking.

In this study, we employ a new black hole solution in the IR regime as a toy gravitational dual model and develop a new computational tool to study the transport coefficients of the normal state of high-temperature superconductors. The radial flow for electric conductivity is derived from the holographic Wilsonian renormalization group equation. The dc conductivity can be read off from the regularity condition at the event horizon. As a toy model toward comparisons with real experimental data, we show that some aspects of the temperature dependence of transport and thermodynamic quantities observed in the experiments can be reproduced in this model. The heat conductivity and Hall Lorenz ratio are proportional to the temperature in the high-temperature regime. The Nernst signal increases as the temperature decreases. Linear temperature resistivity can be obtained at large temperatures, and the Fermi-liquid-like T^2 resistivity is recovered in the low-temperature regime

 © 2017 American Physical Society

with weak momentum relaxation. A key observation is that the transport quantities are governed by the same quantum critical dynamics as those for the thermodynamic quantities. For example, entropy density and specific heat are proportional to temperature, which is similar to the proportionality between resistivity and thermal conductivity under the high-temperature limit. In addition to evaluating the temperature dependence of transport, we compute the Lorenz number and Hall Lorenz ratio at zero temperature.

II. DYONIC BLACK HOLE SOLUTION WITH A HYPERSCALING VIOLATING FACTOR

In this section, we present the details about how to derive a dyonic black hole solution with a dynamic exponent and hyperscaling violating factor in the presence of a magnetic field in four-dimensional bulk spacetime. We consider the Einstein-Maxwell-dilaton-axion model with two $U(1)$ gauge fields. One gauge field coupled with the dilaton field is required to generate a Lifshitz-like vacuum, while the other has a charged black hole. For further investigation of the transport properties, we also add linear axions to generate proper momentum relaxation. Therefore, we consider the following action:

$$S = \int \mathrm{d}^4x\sqrt{-g}\left[R - \frac{1}{2}(\partial\phi)^2 - \frac{1}{4}\sum_{i=1}^{2}\mathrm{e}^{\lambda_i\phi}(F_i)^2 - \frac{1}{2}\mathrm{e}^{\eta\phi}\sum_{i=1}^{2}(\partial\chi_i)^2 + \sum_{i=1}^{2}V_i\mathrm{e}^{\gamma_i\phi}\right], \tag{1}$$

where λ_i, η, γ_i, V_i are undetermined constant parameters and $Z_i(\phi) = \mathrm{e}^{\lambda_i\phi}$, $Y(\phi) = \mathrm{e}^{\eta\phi}$, and $V = V_i\mathrm{e}^{\gamma_i\phi}$.

The equations of motion read

$$R^\mu{}_\nu - \frac{1}{2}\sum_{i=1}^{2}\mathrm{e}^{\lambda_i\phi}(F_i)^{\mu\rho}(F_i)_{\nu\rho} - \frac{1}{2}\mathrm{e}^{\eta\phi}\sum_{i=1}^{2}\partial^\mu\chi_i\partial_\nu\chi_i - \frac{1}{2}\partial^\mu\phi\partial_\nu\phi + \frac{1}{2}\delta^\mu_\nu\left(\frac{1}{4}\sum_{i=1}^{2}\mathrm{e}^{\lambda_i\phi}(F_i)^2 + \sum_{i=1}^{2}V_i\mathrm{e}^{\gamma_i\phi}\right) = 0, \tag{2}$$

$$\partial_\mu(\sqrt{-g}\mathrm{e}^{\lambda_i\phi}(F_i)^{\mu\nu}) = 0, \tag{3}$$

$$\partial_\mu(\sqrt{-g}\mathrm{e}^{\eta\phi}g^{\mu\nu}\partial_\nu\chi_i) = 0, \tag{4}$$

$$\frac{1}{\sqrt{-g}}\partial_\mu(\sqrt{-g}g^{\mu\nu}\partial_\nu\phi) - \frac{1}{4}\sum_{i=1}^{2}\lambda_i\mathrm{e}^{\lambda_i\phi}(F_i)^2 - \frac{1}{2}\eta\mathrm{e}^{\eta\phi}\sum_{i=1}^{2}(\partial\chi_i)^2 + \sum_{i=1}^{2}V_i\gamma_i\mathrm{e}^{\gamma_i\phi} = 0. \tag{5}$$

At the same time, we assume the following ansatz for the metric, gauge fields, and axions:

$$\mathrm{d}s^2 = r^{-\theta}\left(-r^{2z}f(r)\mathrm{d}t^2 + \frac{\mathrm{d}r^2}{r^2f(r)} + r^2\mathrm{d}x^2 + r^2\mathrm{d}y^2\right),$$
$$A_1 = a_1(r)\mathrm{d}t, \qquad A_2 = a_2(r)\mathrm{d}t + Bx\mathrm{d}y,$$
$$\chi_1 = \beta x, \qquad \chi_2 = \beta y,$$

where z and θ are dynamical and hyperscaling violation exponents, respectively [40–42]. The first gauge field A_1 is an auxiliary gauge field, leading to a Lifshitz-like vacuum. The second gauge field is the physical one which provides the finite chemical potential, and B is the magnetic field. From the equations of motion for gauge fields,

$$\partial_r(\sqrt{-g}\mathrm{e}^{\lambda_i\phi}(F_i)^{r\nu}) = 0, \tag{6}$$

we obtain the expression for the charge density,

$$q_i = J_i^t = \sqrt{-g}\mathrm{e}^{\lambda_i\phi}(F_i)^{tr} = r^{-z+3}\mathrm{e}^{\frac{1}{2}\lambda_i\phi}a_i', \tag{7}$$

where q_i are integral constants. According to the holographic principle, q_2 is interpreted as the charge of the black hole, while q_1 is the "charge" associated with the auxiliary $U(1)$ gauge field. The charge q_1 should be vanishing in the case $z = 1$.

Next, subtracting the rr component from the tt component of the Einstein equation (2),

$$-\frac{1}{2}(\theta-2)(\theta-2z+2)r^\theta f + \frac{1}{2}r^{\theta+2}(\phi')^2 f = 0, \tag{8}$$

one can solve the dilaton field,

$$\phi = \sqrt{(\theta-2)(\theta-2z+2)}\ln r = \nu\ln r. \tag{9}$$

The expressions (7) and (9) change the xx component in the Einstein equation (2) to

$$\frac{1}{2}(\theta-2)r^{2\theta-z-1}(r^{-\theta+z+2}f)' - \frac{1}{4}\sum_i r^{-\lambda_i\nu+2\theta-4}(q_i)^2 - \frac{1}{4}r^{\lambda_2\nu+2\theta-4}B^2 - \frac{1}{2}r^{\eta\nu+\theta-2}\nu^2 + \frac{1}{2}\sum_i V_i r^{\gamma_i\nu} = 0. \tag{10}$$

Solving (10), we obtain the function f in terms of some undetermined parameters,

$$f = \sum_i\frac{(q_i)^2r^{-\lambda_i\nu+\theta-4}}{2(\theta-2)(-\lambda_i\nu+z-2)} + \frac{B^2r^{\lambda_2\nu+\theta-4}}{2(\theta-2)(\lambda_2\nu+z-2)} + \frac{\beta^2r^{\eta\nu-2}}{(\theta-2)(\eta\nu-\theta+z)} - \sum_i\frac{V_ir^{\gamma_i\nu-\theta}}{(\theta-2)(\gamma_i\nu-2\theta+z+2)} - mr^{\theta-z-2}, \tag{11}$$

where m is an integral constant related to the mass of the black hole. The condition that the metric is asymptotic

to the Lifshitz geometry fixes the parameter γ_1 as follows:

$$\gamma_1 = \frac{\theta}{\nu}. \tag{12}$$

For the determination of the remaining parameters, we need to use the equation of motion of the dilaton field in which the expressions (7) and (9) are plugged into

$$\begin{aligned}&\nu r^{2\theta-z-1}(r^{-\theta+z+2}f)' + \frac{1}{2}\sum_i \lambda_i r^{-\lambda_i\nu+2\theta-4}(q_i)^2 \\ &\quad -\frac{1}{2}\lambda_2 r^{\lambda_2\nu+2\theta-4}B^2 - \eta r^{\eta\nu+\theta-2}\nu^2 \\ &\quad + \sum_i V_i\gamma_i r^{\gamma_i\nu} = 0.\end{aligned} \tag{13}$$

Combining (10) with (13) by eliminating the function f, one can obtain the following relation

$$\begin{aligned}&\frac{1}{2}\sum_i [\nu + \lambda_i(\theta-2)] r^{-\lambda_i\nu+2\theta-4}(q_i)^2 \\ &\quad + \frac{1}{2}[\nu - \lambda_2(\theta-2)] r^{\lambda_2\nu+2\theta-4}B^2 \\ &\quad + [\nu - \eta(\theta-2)] r^{\eta\nu+\theta-2}\beta^2 \\ &\quad + \sum_i V_i[\gamma_i(\theta-2) - \nu] r^{\gamma_i\nu} = 0.\end{aligned} \tag{14}$$

Since q_2 and β could be arbitrary-valued constants, their coefficients should be zero, and we can determine the values of λ_2 and η. Although B is also arbitrary, its coefficient no longer has an undetermined parameter after λ_2 is determined, so we let the coefficients and the exponentials of the terms which contain B and V_2 be equivalent, respectively. Meanwhile, the q_1 terms should cancel with the V_1 term. In the end, we have

$$\begin{aligned}&\lambda_2 = \frac{\nu}{2-\theta}, \qquad \eta = -\lambda_2 = \frac{\nu}{\theta-2}, \qquad \lambda_1 = \frac{\theta-4}{\nu}, \\ &\gamma_2 = \frac{\theta+2z-6}{\nu}, \qquad q_1^2 = \frac{2V_1(z-1)}{z-\theta+1}, \\ &V_2 = \frac{B^2(2z-\theta-2)}{4(z-2)}.\end{aligned} \tag{15}$$

Since we are considering the effective low-temperature physics of the total geometry, it is not surprising that V_2 depends on the magnetic fields. The magnetic field is fixed in the IR, and only when $2z-\theta=2$, does this term vanish. For example, when $z=1$ and $\theta=0$, V_2 disappears. For simplicity, we introduce the transformation

$$q_2^2 \to 2(\theta-2)(\theta-z)q_2^2, \qquad \beta^2 \to (\theta-2)(z-2)\beta^2. \tag{16}$$

Then, we can plug all parameters (12) and (15) into the expression (11) and obtain the blackening factor

$$\begin{aligned}f &= 1 - mr^{\theta-z-2} + q_2^2 r^{2\theta-2z-2} \\ &\quad + \frac{B^2 r^{2z-6}}{4(z-2)(3z-\theta-4)} - \beta^2 r^{\theta-2z}.\end{aligned}$$

The constant term is set to 1, as long as we demand

$$V_1 = (z-\theta+1)(z-\theta+2). \tag{17}$$

One may notice that as $(z-\theta)\to 0$, $f(r)$ appears to diverge. A well-defined solution can be achieved in an alternative form:

$$\begin{aligned}f(r) &= 1 - \frac{m}{r^{2+z-\theta}} - \frac{q_2^2 \ln r}{2(2-\theta)r^{d+z-\theta}} - \frac{\beta^2}{r^{2z-\theta}} \\ &\quad + \frac{B^2 r^{2z-6}}{4(z-2)(3z-\theta-4)}, \\ &= 1 - \frac{m}{r^2} - \frac{q_2^2 \ln r}{2(2-z)r^2} - \frac{\beta^2}{r^{2z-\theta}} \\ &\quad + \frac{B^2 r^{2z-6}}{4(z-2)(3z-\theta-4)},\end{aligned} \tag{18}$$

$$F_{2rt} = q_2 r^{-1}, \tag{19}$$

where m and q_2 are finite physical parameters without divergence as $(z-\theta)\to 0$. A careful examination of (18) and (19) reveals that they satisfy the corresponding Einstein equation and Maxwell equation. The Hawking temperature at the event horizon $r = r_{\rm H}$ is given by

$$\begin{aligned}T &= \frac{r_{\rm H}^z}{2\pi}\left(1 - \frac{q_2^2}{4(2-z)r_{\rm H}^2} - \frac{\beta^2(2+\theta-2z)}{2r_{\rm H}^{2z-\theta}}\right. \\ &\quad \left. + \frac{B^2 r_{\rm H}^{3z-7}}{4(z-2)(3z-\theta-4)}\right).\end{aligned} \tag{20}$$

As $z\to 1$ and $\theta\to 1$, the first auxiliary gauge field then vanishes, and the metric of the black hole solution can be recast as

$$\begin{aligned}ds^2 &= -g_{tt}dt^2 + g_{rr}dr^2 + g_{xx}(dx^2+dy^2) \\ &= r^{-\theta}\left[-r^2 f(r)dt^2 + \frac{dr^2}{r^2 f(r)} + r^2(dx^2+dy^2)\right], \\ f(r) &= 1 - \frac{m}{r^2} - \frac{q_2^2 \ln r}{2r^2} - \frac{\beta^2}{r} + \frac{B^2}{8r^4}, \\ A &= q_2 \ln r dt + \frac{B}{2}(xdy - ydx), \\ e^{\phi} &= r, \qquad \chi_i = \beta\delta_{ia}x^a, \\ V(\phi) &= 2r + B^2 r^{-3}/8, \\ Z(\phi) &= r^{-1}, \qquad Y(\phi) = r,\end{aligned} \tag{21}$$

where θ, m, q, and B are the parameters related to the hyperscaling violation factor, mass, charge, and magnetic field, respectively. Equation (21) is the main metric ansatz

used in this paper. Note that the magnetic field B appears in the potential $V(\phi)$ because we only consider the IR geometry here so that the magnetic field is fixed in the action. One critical observation is that in the absence of β and B terms, the blacken function $f(r)$ and the scalar potential A_t are the same as those of the $(2+1)$-dimensional charged BTZ black brane [43–45]. The electrostatic potential of the black hole diverges asymptotically as $\ln r$. But the presence of divergent boundary terms is an artifact of the renormalization procedure, and the divergence can be removed [46]. The boundary is located at $r \to +\infty$. The nondegenerate horizon is located at $r = r_{\rm H}$, where $f(r_{\rm H}) = 0$ and its associated Hawking temperature is given by

$$T = \frac{r_{\rm H}}{2\pi}\left(1 - \frac{q_2^2}{4r_{\rm H}^2} - \frac{\beta^2}{2r_{\rm H}} - \frac{B^2}{8r_{\rm H}^4}\right). \tag{22}$$

The black hole solution is not an asymptotic AdS solution; therefore, it can, in principle, be interpreted as an IR geometry embedded in the AdS space. When $r_{\rm H} \gg \beta^2$, $r_{\rm H}^2 \gg q_2^2$ and $r_{\rm H}^4 \gg B^2$, we recover the well-known relativistic scaling $T \sim r_{\rm H}$. This corresponds to a large temperature regime, although the temperature satisfying these ranges can be decreased by tuning β, q_2, and B. The entropy density and the specific heat of this black hole are given by $s = 4\pi r_{\rm H}$ and

$$c_{q_2,\beta,B} = T\left(\frac{\partial s}{\partial T}\right)_{q_2,\beta,B} = 4\pi^2\left(1 + \frac{\beta^2 + 4\pi T}{\sqrt{4q_2^2 + (\beta^2 + 4\pi T)^2}}\right).$$

These are proportional to the temperature in the large-temperature regime. Experiments on optimally doped $YBa_2CuO_{7-\delta}$ provide the electronic specific heat $c \sim T$ from critical to room temperatures [47]. As shown in the following, this Fermi-liquid scaling is not in conflict with that of the anomalous transport.

The electric charge density is $q_2 \equiv -J^t = -\sqrt{-g}Z(\phi)\partial_r A_t$. At zero temperature, that is, when $T = 0$, the solution near the horizon develops an $AdS_2 \times R^2$ geometry. The near-horizon geometry reads $ds^2 \sim u^{-2}(-dt^2 + du^2) + r_{\rm H}^2(dx^2 + dy^2)$, where $u = r_{\rm H}^2/(r - r_{\rm H})$. The Hawking temperature shows that even in the absence of the $U(1)$ gauge field, the black hole could still be extremal with a near-horizon geometry of AdS_2. This implies that at low temperatures, the theory flows to an infrared fixed point in the presence of linear axion fields. However, a near-extremal dyonic black hole is unstable to forming neutral scalar hair. From the holographic dictionary point of view, we expect there is a domain wall solution interpolating between AdS_4 in the UV and dyonic $AdS_2 \times R^2$ solutions in the IR. In [48], dyonic black holes at finite temperature approaching AdS_4 in the UV were constructed. If the scalar field is above the BF bound for AdS_4 but below the Breitenlohner-Freedman bound for AdS_2, the black hole becomes unstable near extremality. For big enough magnetism, the black hole approaches hyperscaling violating behavior in the IR as $T \to 0$ [48].

III. HOLOGRAPHIC TRANSPORT COEFFICIENTS

The transport coefficients are computed in the holography by studying perturbations of the background solution. We developed the holographic Wilsonian approach previously given in [49–53] and computed the dc conductivity by applying linear sources to the boundary fields. As far as we know, the Wilsonian renormalization group approach has not been utilized to describe the radial flow for transport coefficients in the presence of momentum dissipation. For computing the transport coefficients, the consistent perturbation ansatz reads

$$\delta A_{x_i} = \int_{-\infty}^{\infty} \frac{d\omega}{2\pi} e^{-i\omega t} a_i(\omega, r), \tag{23}$$

$$\delta g_{tx_i} = \int_{-\infty}^{\infty} \frac{d\omega}{2\pi} e^{-i\omega t} g_{xx} h_{tx_i}(\omega, r), \tag{24}$$

$$\delta \chi_i = \int_{-\infty}^{\infty} \frac{d\omega}{2\pi} e^{-i\omega t} \chi_i(\omega, r), \tag{25}$$

where i runs over (1,2), and $x_1 = x$ and $x_2 = y$. We notice that in the computation of conductivity, we also need to perturb the potential, but the B^2 term does not contribute to the equations of motion as we can see δA_{x_i} is only a function of r and t. Since the spatial $SO(2)$ is unbroken, it is convenient to organize the fields as

$$a_z = \frac{(a_x - ia_y)}{2}, \qquad h_{tz} = \frac{(h_{tx} - ih_{ty})}{2},$$
$$\chi_z = \frac{(\chi_x - i\chi_y)}{2}.$$

We can define a matrix $\tilde{\sigma}$ from

$$[\![\begin{matrix} \sqrt{g_{tt}/g_{rr}} \\ Za_z' g_{xx}^2/\sqrt{g_{rr}g_{tt}}h_{tz}' \\ \sqrt{g_{tt}/g_{rr}} Z g_{xx}\chi_z' \end{matrix}]\!] = \tilde{\sigma}[\![\begin{matrix} i\omega a_z \\ i\omega h_{tz} \\ i\omega \chi_z \end{matrix}]\!],$$

where the special notation $[\![\ldots]\!]$ is what we introduced just for convenience, for example,

$$[\![\begin{matrix} a_z \\ h_{tz} \\ \chi_z \end{matrix}]\!] \equiv \begin{pmatrix} a_z & a_z^{(2)} & a_z^{(3)} \\ h_{tz} & h_{tz}^{(2)} & h_{tz}^{(3)} \\ \chi_z & \chi_z^{(2)} & \chi_z^{(3)} \end{pmatrix}, \tag{26}$$

where $a_z^{(i)}$, $h_{tz}^{(i)}$, and $\chi_z^{(i)}$ are linearly independent source vectors, introduced to guarantee the source term is

invertible. The RG flow equation of $\tilde{\sigma}$ can be obtained by taking the derivative of $\tilde{\sigma}$ (see Appendix B for details) [54]:

$$\tilde{\sigma}' = \frac{Z\sqrt{g_{rr}/g_{tt}}}{i\omega}\begin{pmatrix} -\omega^2 & \omega B & 0 \\ -\omega B & g_{xx}Y\beta^2 + B^2 & i\omega g_{xx}Y\beta^2 \\ 0 & i\omega g_{xx}Y(\phi)\beta^2 & -\omega^2 g_{xx} \end{pmatrix} - i\omega\sqrt{\frac{g_{rr}}{g_{tt}}}\tilde{\sigma}\begin{pmatrix} 1/Z & 0 & 0 \\ 0 & g_{tt}/g_{xx}^2 & 0 \\ 0 & 0 & \frac{1}{g_{xx}Z} \end{pmatrix}\tilde{\sigma} + \begin{pmatrix} 0 & \frac{\sqrt{g_{rr}g_{tt}}}{g_{xx}} & 0 \\ \frac{q_2}{Z}\frac{g_{rr}}{g_{tt}} & g_{tt}/g_{xx}^2 & 0 \\ 0 & 0 & \frac{1}{g_{xx}Z} \end{pmatrix}\tilde{\sigma}.$$

The advantage of the holographic Wilsonian approach is that it reduces the computation of conductivity from second-order ordinary differential equations to first-order nonlinear ordinary differential equations. The regularity condition at the event horizon gives the boundary condition

$$\tilde{\sigma}_0 = \begin{pmatrix} Z & -\frac{ZB}{\omega} & 0 \\ \frac{BZ - iq_2}{\omega} & \sigma_{22} & -\frac{i\beta g_{xx}Y}{\omega} \\ -\frac{i\beta g_{xx}Y}{\omega} & 0 & g_{xx}Y \end{pmatrix}.$$

From the definition of the matrix $\tilde{\sigma}$, we obtain the boundary condition at the event horizon,

$$\sqrt{\frac{g_{tt}}{g_{rr}}}a_z' \to i\omega a_z - iBh_{tz}|_{r=r_{\rm H}}. \tag{27}$$

Finally, we obtain the expressions for h_{tx} and h_{ty} at the event horizon,

$$h_{tx} = -i\omega\frac{a_x g_{xx}q_2\beta^2 Y + a_y B(q_2^2 + B^2Z^2 + g_{xx}Z\beta^2 Y)}{(B^2Z + g_{xx}\beta^2 Y)^2 + B^2q_2^2} - i\omega\frac{Bg_{xx}Y\chi_y + (B^2 g_{xx}YZ + g_{xx}^2 Y\beta^2)\chi_x}{(B^2Z + g_{xx}\beta^2 Y)^2 + B^2q_2^2}\bigg|_{r=r_{\rm H}},$$

$$h_{ty} = i\omega\frac{a_x B(q_2^2 + B^2Z^2 + g_{xx}Z\beta^2 Y) - a_y g_{xx}q_2\beta^2 Y}{(B^2Z + g_{xx}\beta^2 Y)^2 + B^2q_2^2} + i\omega\frac{Bg_{xx}Y\chi_x - (B^2 g_{xx}YZ + g_{xx}^2 Y\beta^2)\chi_y}{(B^2Z + g_{xx}\beta^2 Y)^2 + B^2q_2^2}\bigg|_{r=r_{\rm H}}.$$

The radially conserved currents can be deduced from the Maxwell equation,

$$J_x = i\omega Za_x - q_2h_{tx} - ZBh_{ty},$$
$$J_y = i\omega Za_y - q_2h_{ty} + ZBh_{tx}. \tag{28}$$

An important step in the evaluation of thermoelectric and heat conductivity tensors involves the determination of physical quantities that are independent of the radial coordinate. The conductivity tensor can be evaluated using $\sigma_{ij} = \partial J_i/\partial E_j$ with $E_j = -i\omega a_j$. The electrical conductivity tensor reads

$$\sigma_{xx} = \sigma_{yy} = \frac{\beta^2 r_{\rm H}^2(B^2 + q_2^2 r_{\rm H}^2 + \beta^2 r_{\rm H}^3)}{B^4 + \beta^4 r_{\rm H}^6 + B^2 r_{\rm H}^2(q_2^2 + 2\beta^2 r_{\rm H})}, \tag{29}$$

$$\sigma_{xy} = -\sigma_{yx} = \frac{Bq_2(B^2 + q_2^2 r_{\rm H}^2 + 2\beta^2 r_{\rm H}^3)}{B^4 + \beta^4 r_{\rm H}^6 + B^2 r_{\rm H}^2(q_2^2 + 2\beta^2 r_{\rm H})}. \tag{30}$$

Notably, in the absence of the external magnetic field, the dc electric conductivity along the x direction is separated into two terms,

$$\sigma_{xx} \sim \frac{1}{2\pi T} + \frac{q_2^2}{4\pi^2\beta^2 T^2}. \tag{31}$$

The corresponding resistivity in the small β limit can be written as

$$\rho_{xx} \simeq \frac{4\beta^2\pi^2 T^2}{q_2^2 + 2\beta^2\pi T} = \frac{\tilde{T}^2}{\tilde{T} + \Delta}, \tag{32}$$

where we defined $\tilde{T} = 2\pi T$ and $\Delta = q_2^2/\beta^2$. For $\tilde{T} \gg \Delta$, the corresponding resistivity is dominated by the linear-T behavior, whereas in the low-temperature regime, $\tilde{T} \ll \Delta$, the system supports Landau's Fermi-liquid T^2 law. On the other hand, in the strong external magnetic field limit (i.e., $B \gg q_2, \beta$) and in the small-temperature limit, the electric resistivity can be approximated as

$$\rho_{xx} = \frac{\beta^2 r_{\rm H}^2[B^2q_2^2 + r_{\rm H}^2(q_2^2 + \beta^2 r_{\rm H})]}{B^2 + r_{\rm H}^2(q_2^2 + \beta^2 r_{\rm H})^2} \sim \frac{\beta^2}{q_2^2}r_{\rm H}^2 \sim 0.35B\frac{\beta^2}{q_2^2} + 1.86T\sqrt{B}\frac{\beta^2}{q_2^2} + 2.46T^2\frac{\beta^2}{q_2^2} + \mathcal{O}(T^3). \tag{33}$$

Since the quadratic temperature dependence of inverse Hall angles has been observed in multiple cuprates in the underdoped to overdoped regions [1], the calculation of the Hall angle in holography is also an interesting topic. The Hall angle $\cot\vartheta_H \equiv \sigma_{xx}/\sigma_{xy}$, in this model, is found to be

$$\cot\vartheta_H \sim \frac{\beta^2 r_{\rm H}^2}{Bq_2} \sim T^2. \tag{34}$$

Thus, we give an explicit model realizing the anomalous scaling of the Hall angle proposed in Ref. [8]. That is to say, the Hall relaxation rate is different from the transport scattering rate of the linear-in-temperature resistivity. Below, we also calculate other transport coefficients such

as thermo-electric conductivities, thermal conductivity, and Lorenz constants.

The conserved heat currents $\mathcal{Q}^i$ are defined by introducing a two-form associated with the Killing vector field equation $K = \partial_t$, as follows [14,15]:

$$\mathcal{Q}^i = \sqrt{\frac{g_{tt}}{g_{rr}}}\left(-\frac{g'_{tt}}{g_{tt}} g_{ii}\delta h_{ti} + g'_{ii}\delta h_{ti} + g_{ii}\delta h'_{tx}\right) - A_t J^i + M(r)\epsilon_{ij}E_j + 2M_Q(r)\epsilon_{ij}\zeta_j, \tag{35}$$

where

$$M(r) = \int_{r_H}^{r} dx g^{xx} Z(\phi) B, \tag{36}$$

and

$$M_Q(r) = \int_{r_H}^{r} dr' g^{xx} Z(\phi) B A_t(r'). \tag{37}$$

Note that $M(r)$ and $M_Q(r)$ correspond to the magnetization density of the boundary theory as $r \to \infty$. The aforementioned ansatz corresponds to the application of an external electric field E_i along the x_i direction and the temperature gradient $(\nabla T)_i = \zeta_i T$ to the boundary theory. As the heat currents $\mathcal{Q}^i$ are radially conserved, we can evaluate them at the event horizon,

$$\mathcal{Q}^x = -\sqrt{\frac{g_{tt}}{g_{rr}}}\frac{g'_{tt}}{g_{tt}} g_{xx}\delta h_{tx}\bigg|_{r=r_H},$$
$$\mathcal{Q}^y = -\sqrt{\frac{g_{tt}}{g_{rr}}}\frac{g'_{tt}}{g_{tt}} g_{xx}\delta h_{ty}\bigg|_{r=r_H}. \tag{38}$$

The electrothermal conductivity can be evaluated at the event horizon as

$$\alpha_{xx} = \alpha_{yy} = \frac{\partial \mathcal{Q}^x}{T\partial E_x} = \frac{4\pi q_2 \beta^2 r_H^5}{B^2 q_2^2 r_H^2 + (B^2 + \beta^2 r_H^3)^2},$$
$$\alpha_{xy} = -\alpha_{yx} = \frac{\partial \mathcal{Q}^y}{T\partial E_x} = \frac{4\pi B r_H (q_2^2 r_H^2 + B^2 + r_H^3\beta^2)}{B^2 q_2^2 r_H^2 + (B^2 + \beta^2 r_H^3)^2}. \tag{39}$$

Finally, we can extract the heat conductivity tensor as

$$\bar{\kappa}_{xx} = \bar{\kappa}_{yy} = \frac{16\pi^2 T r_H^3 (B^2 + \beta^2 r_H^3)}{B^2 q_2^2 r_H^2 + (B^2 + \beta^2 r_H^3)^2}, \tag{40}$$

$$\bar{\kappa}_{xy} = -\bar{\kappa}_{yx} = \frac{16\pi^2 T B q_2 r_H^4}{B^2 q_2^2 r_H^2 + (B^2 + \beta^2 r_H^3)^2}. \tag{41}$$

The usual thermal conductivity that is more readily measurable experimentally is defined by introducing the thermal conductivity at zero electric current, $\kappa_{xx} = \bar{\kappa}_{xx} - \alpha_{xx}\bar{\alpha}_{xx}T/\sigma_{xx}$,

$$\kappa_{xx} = \frac{16\pi^2 r_H^3 T}{B^2 + r_H^2(q_2^2 + \beta^2 r_H)}. \tag{42}$$

In the large-temperature regime, the heat conductivity $\kappa_{xx} \sim T$, which is same as the specific heat.

Next, we evaluate the Hall Lorenz ratio as follows:

$$\bar{L}_H \equiv \frac{\bar{\kappa}_{xy}}{T\sigma_{xy}} = \frac{16\pi^2 r_H^4}{B^2 + q_2^2 r_H^2 + \beta^2 r_H^3}. \tag{43}$$

At high temperature, the Hall Lorenz ratio behaves as $\bar{L}_H \sim T$. This temperature dependence can be compared with the experimental results in [55]. At zero temperature, with a vanishing magnetic field, the Hall Lorenz ratio becomes $\bar{L}_H = 4\pi^2 + \frac{4\pi^2\beta^2}{\sqrt{4q_2^2+\beta^4}}$.

Since the Nernst signal in cuprates has significantly different behaviors compared with conventional metals, we examine the Nernst signal holographically

$$e_N \equiv (\sigma^{-1}\cdot\alpha)_{xy} = \frac{4\pi B r_H^3 \beta^2}{B^2 q_2^2 + r_H^2(q_2^2 + r_H\beta^2)^2} \sim \frac{4\pi}{\beta^2 T} + \mathcal{O}\left(\frac{1}{T^2}\right), \tag{44}$$

where σ and α denote the electric and thermoelectric conductivity matrices, respectively. Figure 1 shows that the Nernst signal increases as temperature decreases at the high-temperature limit. Moreover, as shown in Fig. 2, the obtained Nernst signal demonstrates a bell-shaped dependence on the magnetic field. The blue line is almost straight, whereas the green and red lines yield hill profiles. Our system shows the transition from typical metal (blue line) to the cuprate state (green, purple, and red), as the disorder β decreases in the Nernst signal perspective. Comparisons can be made between the results obtained here and experimental data presented in [56–58]. For example, the

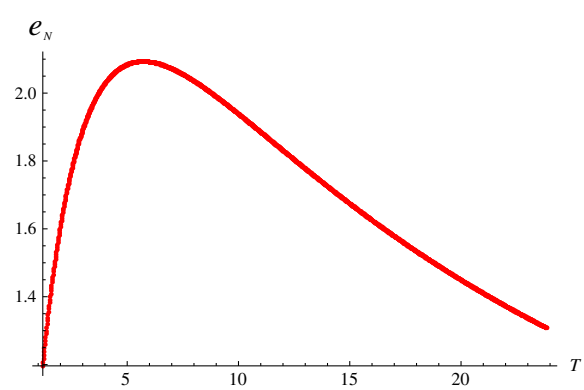

FIG. 1. Nernst signal as a function of temperature with $q_2 = 3$, $\beta = 1/2$, and $B = 5$.

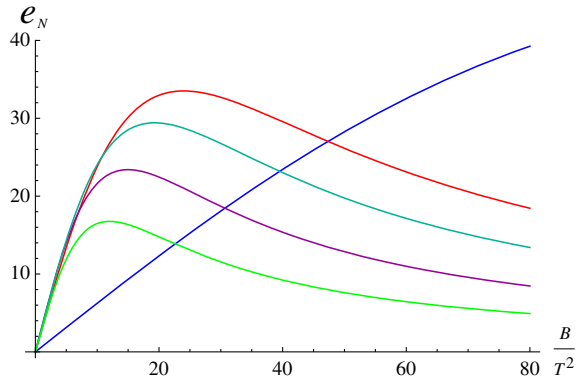

FIG. 2. Nernst signal as a function of magnetic field B. The lines from the top to bottom correspond to $\beta/T = 1$, 0.84, 0.66, 0.5, 1.5.

"hill" profile shown in Figs. 1 and 2 is similar to those in Figs. 5, 6, 9, and 12 in [56]. But the scaling behavior of the Nernst signal is not clear from the existing literature.

Moreover, we are able to consider the thermoelectric power (Seebeck coefficient)

$$S \equiv \frac{\alpha_{xx}}{\sigma_{xx}} = \frac{4\pi q_2 r_{\mathrm{H}}^3}{B^2 + r_{\mathrm{H}}^2(q_2^2 + \beta^2 r_{\mathrm{H}})}. \tag{45}$$

Under the weak magnetic field and charge limit, S behaves as a constant. But in the small disorder limit, keeping q_2 and B fixed, we have $S \sim T$ as r_{H} becomes large. The experimental result obtained at optimal doping suggested the relation $S \sim a - bT$, where a, b are constants [1]. However, there is no consensus on the temperature scaling of the thermoelectric power from the experimental data [59], even though some data appear to show a negative slope.

The Lorenz constant L, which is related to the Wiedemann-Franz law, is a key signature of a Fermi liquid. In general, if $L/L_0 = 1$ $(L_0 = \pi^2/3 \times k_B^2/e^2)$ at zero temperature, Landau's Fermi-liquid description is satisfied. In [60], $L/L0 \gg 1$ has been used to diagnose strong deviations from the quasiparticle picture in graphene. On the other hand, $L/L_0 < 1$ at zero temperature also indicates the breakdown of the Fermi-liquid theory [61–63].

At zero temperature and under a vanishing magnetic field, the Lorenz ratio is given by

$$L = \left.\frac{\kappa_{xx}}{T\sigma_{xx}}\right|_{T,B\to 0} = 4\pi^2 \frac{\beta^4}{4q_2^2 + \beta^4} + \frac{4\pi^2\beta^2}{\sqrt{4q_2^2 + \beta^4}}. \tag{46}$$

Therefore, at $B = 0$, the Lorenz number becomes $8\pi^2$ only when the disorder becomes stronger (i.e., $\beta^4/q_2^2 \to \infty$). As $\beta^4/q_2^2 \to 0$, the Lorenz number approaches zero, and deviations from the Fermi-liquid behavior can be observed. A Lorenz ratio at zero temperature is comparable with the Hall Lorenz ratio given in (43),

$$\bar{L} = \left.\frac{\bar{\kappa}_{xx}}{T\sigma_{xx}}\right|_{T,B\to 0} = 4\pi^2 + \frac{4\pi^2\beta^2}{\sqrt{4q_2^2 + \beta^4}}. \tag{47}$$

The Hall Lorenz ratio $\bar{L}_H$ at zero temperature under the weak magnetic field with finite q_2 and β limits exactly equals $\bar{L}$ obtained in this study. In the large-temperature regime, the Lorenz ratios $\bar{L}$ and L presented here are also proportional to the temperature, same as $\bar{L}_H$.

IV. DISCUSSIONS AND CONCLUSIONS

In summary, we started from the general Einstein-Maxwell-axion-dilaton theory, an effective low-temperature theory, in four-dimensional spacetime and obtained a dyonic black hole solution with a nonzero hyperscaling violating factor. The temperature dependence of thermodynamic quantities such as entropy density and specific heat were obtained in the small β, q_2, and B limit. Since the metric represents the low-temperature part of the geometry and can be connected to a UV AdS_4 geometry, the thermodynamic quantities expanded in the high-temperature part make sense in the calculations.

We then computed the transport coefficients in this holographic model. Linear-temperature-dependence resistivity and quadratic-temperature-dependence inverse Hall angle were achieved. Temperature scaling of the Hall Lorenz ratio and Nernst signal are also calculated in this model. The dc transport quantities obtained here are governed by the same quantum critical dynamics as those for the thermodynamic quantities of the black hole. These results can be compared to that of cuprate strange metals. It seems that, by exploring a new black hole solution with dynamical exponent $z = 1$ and hyperscaling violation exponent $\theta = 1$, one can reproduce different temperature scalings of the anomalous transport observed in experiments. However, the results were obtained by introducing an extra scale related to β^2 and to the scaling dimension of the operator breaking translations. More precisely, a particular combination of β^2, q_2, B, and T leads to (33), as do the heat conductivity, the Hall Lorenz ratio, and the Nernst signal. Therefore, the results cannot be directly compared to [36,38]. In the future, it would be interesting to compute numerical optical conductivities and the onset of superconductivity in this holographic model.

ACKNOWLEDGMENTS

We would like to thank the anonymous referees for valuable comments and suggestions. The authors would also like to thank Glenn Barnich, John Mcgreevy, Sang-Jin Sin, and Elias Kiritsis for helpful discussions. The study was partially supported by NSFC China (Grant No. 11375110); NSFC Grant No. 11475179 and Grant No. 14DZ2260700 from Shanghai Key Laboratory of High Temperature Superconductors; the Ministry of Science and Technology (Grant No. MOST 104-2811-M-009-068) and

National Center for Theoretical Sciences in Taiwan; and by NSFC China (Grant No. 11275120).

APPENDIX: NEW ANALYTIC METHOD ON TRANSPORT COEFFICIENTS

It was proved in [51] that several approaches to RG flow of transport coefficients are equivalent: These approaches include the sliding membrane paradigm [49], Wilsonian fluid/gravity [53], and holographic Wilsonian RG [50]. The essential idea of the holographic Wilsonian renormalization group approach is to integrate out the bulk field from the boundary up to some intermediate radial distance. The radial direction in the bulk marks the energy scale of the boundary theory, and the radial flow in the bulk geometry can be interpreted as the renormalization group flow of the boundary theory.

The equations of motion of the linear perturbation are given by

$$\begin{aligned}
&\left(\frac{g_{xx}^2}{\sqrt{g_{rr}g_{tt}}}h_{tz}'\right)' - q_2 a_z' - \beta^2 g_{xx} Y\sqrt{\frac{g_{rr}}{g_{tt}}}h_{tz} \\
&\quad - i\omega g_{xx} Y\sqrt{\frac{g_{rr}}{g_{tt}}}\chi_z + \omega BZ\sqrt{\frac{g_{rr}}{g_{tt}}}a_z - B^2 Z\sqrt{\frac{g_{rr}}{g_{tt}}}h_{tz} = 0, \\
&\left(\sqrt{\frac{g_{tt}}{g_{rr}}}Z a_z'\right)' - q_2 h_{tz}' + \omega^2 Z\sqrt{\frac{g_{rr}}{g_{tt}}}a_z - \omega BZ\sqrt{\frac{g_{rr}}{g_{tt}}}h_{tz} = 0, \\
&\left(\sqrt{\frac{g_{tt}}{g_{rr}}}g_{xx} Y\chi_z'\right)' + \omega^2 Y g_{xx}\sqrt{\frac{g_{rr}}{g_{tt}}}\chi_z - i\omega\beta^2 Y g_{xx}\sqrt{\frac{g_{rr}}{g_{tt}}} \\
&h_{tz} = 0, \\
&\frac{\omega g_{xx}^2}{\sqrt{g_{rr}g_{tt}}}h_{tz}' - B\sqrt{\frac{g_{tt}}{g_{rr}}}a_z' + i\beta g_{xx} Y\sqrt{\frac{g_{tt}}{g_{rr}}}a_z' + Bq_2 h_{tz} \\
&\quad - \omega q_2 a_z = 0.
\end{aligned} \tag{A1}$$

In order to deduce the RG flow equation of the transport, we define a matrix $\tilde{\sigma}$ by assuming

$$\begin{bmatrix} \sqrt{g_{tt}/g_{rr}}Z a_z' \\ g_{xx}^2/\sqrt{g_{rr}g_{tt}}h_{tz}' \\ \sqrt{g_{tt}/g_{rr}}Z g_{xx}\chi_z' \end{bmatrix} = \tilde{\sigma}\begin{bmatrix} i\omega a_z \\ i\omega h_{tz} \\ i\omega\chi_z \end{bmatrix},$$

where we have introduced the notation

$$\begin{bmatrix} a_z \\ h_{tz} \\ \chi_z \end{bmatrix} \equiv \begin{pmatrix} a_z & a_z^{(2)} & a_z^{(3)} \\ h_{tz} & h_{tz}^{(2)} & h_{tz}^{(3)} \\ \chi_z & \chi_z^{(2)} & \chi_z^{(3)} \end{pmatrix}, \tag{A2}$$

with $a_z^{(i)}$, $h_{tz}^{(i)}$, and $\chi_z^{(i)}$ linearly independent source vectors obeying the same equation as (A2). These auxiliary vectors are only introduced to make the source term a square matrix. So the notation $[\![\ldots]\!]$ is invertible in the following derivation, while the column matrix on the left-hand side should also be understood in the same sense. Taking the derivative of $\tilde{\sigma}$ and using the EoM repetitiously, we obtain

$$\begin{aligned}
\tilde{\sigma}' &= \begin{bmatrix} \sqrt{g_{tt}/g_{rr}}Z a_z' \\ g_{xx}^2/\sqrt{g_{rr}g_{tt}}h_{tz}' \\ \sqrt{g_{tt}/g_{rr}}Z g_{xx}\chi_z' \end{bmatrix}\begin{bmatrix} i\omega a_z \\ i\omega h_{tz} \\ i\omega\chi_z \end{bmatrix}^{-1} \\
&\quad - i\omega\tilde{\sigma}\begin{bmatrix} a_z' \\ h_{tz}' \\ \chi_z' \end{bmatrix}\begin{bmatrix} i\omega a_z \\ i\omega h_{tz} \\ i\omega\chi_z \end{bmatrix}^{-1} \\
&= \frac{\sqrt{g_{rr}/g_{tt}}}{i\omega}\begin{pmatrix} -\omega^2 Z & \omega BZ & 0 \\ -\omega BZ & g_{xx}Y\beta^2 + B^2 Z & i\omega g_{xx}Y\beta^2 \\ 0 & i\omega g_{xx}Y\beta^2 & -\omega^2 g_{xx}Y \end{pmatrix} \\
&\quad - i\omega\sqrt{\frac{g_{rr}}{g_{tt}}}\tilde{\sigma}\begin{pmatrix} \frac{1}{Z} & 0 & 0 \\ 0 & \frac{g_{tt}}{g_{xx}^2} & 0 \\ 0 & 0 & \frac{1}{g_{xx}Z} \end{pmatrix}\tilde{\sigma} \\
&\quad + \begin{pmatrix} 0 & \frac{\sqrt{g_{rr}g_{tt}}}{g_{xx}} & 0 \\ \frac{q_2}{Z}\sqrt{\frac{g_{rr}}{g_{tt}}} & 0 & 0 \\ 0 & 0 & 0 \end{pmatrix}\tilde{\sigma}.
\end{aligned}$$

The prime denotes the derivative with respect to r. At the event horizon, $g_{tt}/g_{rr} \to 0$ and $g_{tt}\sigma'/g_{rr} \to 0$, the regularity condition then requires

$$\tilde{\sigma}_0 = \begin{pmatrix} Z & -\frac{ZB}{\omega} & 0 \\ \frac{BZ - iq_2}{\omega} & \sigma_{22} & -\frac{i\beta g_{xx}Y}{\omega} \\ -\frac{i\beta g_{xx}Y}{\omega} & 0 & g_{xx}Y \end{pmatrix}. \tag{A3}$$

Note that σ_{22} can be determined by the constraint equation (A2), which can be written as

$$\begin{pmatrix} 0 & 0 & 0 \\ -iB & i\omega & -\beta \\ 0 & 0 & 0 \end{pmatrix}\tilde{\sigma} = \begin{pmatrix} 0 & 0 & 0 \\ q_2 & -Bq_2/\omega & 0 \\ 0 & 0 & 0 \end{pmatrix}.$$

The above equation leads to

$$-iB\tilde{\sigma}_{11} + i\omega\tilde{\sigma}_{21} - \beta\tilde{\sigma}_{31} = q_2, \tag{A4}$$

$$-iB\tilde{\sigma}_{12} + i\omega\tilde{\sigma}_{22} - \beta\tilde{\sigma}_{32} = -\frac{Bq_2}{\omega}, \tag{A5}$$

$$-iB\tilde{\sigma}_{13} + i\omega\tilde{\sigma}_{23} - \beta\tilde{\sigma}_{33} = 0. \tag{A6}$$

From (A5), we obtain

$$\tilde{\sigma}_{22} = \frac{iBq_2}{\omega^2} - \frac{ZB^2 + g_{xx}Y\beta^2}{\omega^2}. \tag{A7}$$

Equations (A4) and (A6) are evidently satisfied by components of $\tilde{\sigma}_0$ given in (A3). Therefore, from the definition of $\tilde{\sigma}$, we have the regularity condition at the event horizon,

$$\sqrt{\frac{g_{tt}}{g_{rr}}}a_z' \to i\omega a_z - iBh_{tz}|_{r=r_\mathrm{H}}. \tag{A8}$$

Together with the regularity condition for h_{tz} from the first equation of (A2), we arrive at

$$\begin{aligned}&(\beta^2 g_{xx}Y + B^2 Z - iBq_2)h_{tz}|_{r=r_\mathrm{H}}\\ &\quad = (\omega BZ - i\omega q_2)a_z|_{r=r_\mathrm{H}} - i\omega g_{xx}Y\chi_z|_{r=r_\mathrm{H}}.\end{aligned}$$

Keeping in mind that $h_{tz} = (h_{tx} - ih_{ty})/2$ and $\chi_z = (\chi_x - i\chi_y)/2$, we easily obtain

$$\begin{aligned}h_{tx} &= -i\omega\frac{a_x g_{xx}q_2\beta^2 Y + a_y B(q_2^2 + B^2Z^2 + g_{xx}Z\beta^2 Y)}{(B^2Z + g_{xx}\beta^2 Y)^2 + B^2q_2^2}\\ &\quad - \left.\frac{Bg_{xx}Y\chi_y + (B^2 g_{xx}YZ + g_{xx}^2 Y\beta^2)\chi_x}{(B^2Z + g_{xx}\beta^2 Y)^2 + B^2q_2^2}\right|_{r=r_\mathrm{H}},\\ h_{ty} &= i\omega\frac{a_x B(q_2^2 + B^2Z^2 + g_{xx}Z\beta^2 Y) - a_y g_{xx}q_2\beta^2 Y}{(B^2Z + g_{xx}\beta^2 Y)^2 + B^2q_2^2}\\ &\quad + \left.\frac{Bg_{xx}Y\chi_x - (B^2 g_{xx}YZ + g_{xx}^2 Y\beta^2)\chi_y}{(B^2Z + g_{xx}\beta^2 Y)^2 + B^2q_2^2}\right|_{r=r_\mathrm{H}}.\end{aligned}$$

One can simply drop the χ_i terms in the expressions for h_{tx} and h_{ty} since these terms do not contribute to the transport coefficients as shown below. The radially conserved currents can be deduced from the Maxwell equation,

$$\begin{aligned}J_x &= i\omega Za_x - q_2 h_{tx} - ZBh_{ty},\\ J_y &= i\omega Za_y - q_2 h_{ty} + ZBh_{tx}.\end{aligned} \tag{A9}$$

The dc electric conductivity can be calculated via $\sigma_{ij} = \frac{\partial J_i}{\partial E_j}$, where $E_j = -i\omega a_j$. The electrical conductivity tensor then reads

$$\begin{aligned}\sigma_{xx} = \sigma_{yy} &= \frac{\beta^2 r_\mathrm{H}^2(B^2 + q_2^2 r_\mathrm{H}^2 + \beta^2 r_\mathrm{H}^3)}{B^4 + \beta^4 r_\mathrm{H}^6 + B^2 r_\mathrm{H}^2(q_2^2 + 2\beta^2 r_\mathrm{H})},\\ \sigma_{xy} = -\sigma_{yx} &= \frac{Bq_2(B^2 + q_2^2 r_\mathrm{H}^2 + 2\beta^2 r_\mathrm{H}^3)}{B^4 + \beta^4 r_\mathrm{H}^6 + B^2 r_\mathrm{H}^2(q_2^2 + 2\beta^2 r_\mathrm{H})}.\end{aligned}$$

The radially conserved heat currents are given by

$$\begin{aligned}\mathcal{Q}^x &= -\sqrt{\frac{g_{tt}}{g_{rr}}}\frac{g_{tt}'}{g_{tt}}g_{xx}\delta h_{tx}|_{r=r_\mathrm{H}},\\ \mathcal{Q}^y &= -\sqrt{\frac{g_{tt}}{g_{rr}}}\frac{g_{tt}'}{g_{tt}}g_{xx}\delta h_{ty}|_{r=r_\mathrm{H}}.\end{aligned} \tag{A10}$$

Thus, we can evaluate the electrothermal conductivity matrix as

$$\begin{aligned}\alpha_{xx} = \alpha_{yy} &= \frac{\partial\mathcal{Q}^x}{T\partial E_x} = \frac{4\pi q_2\beta^2 r_\mathrm{H}^5}{B^2q_2^2r_\mathrm{H}^2 + (B^2 + \beta^2 r_\mathrm{H}^3)^2},\\ \alpha_{xy} = -\alpha_{yx} &= \frac{\partial\mathcal{Q}^y}{T\partial E_x} = \frac{4\pi Br_\mathrm{H}(q_2^2r_\mathrm{H}^2 + B^2 + r_\mathrm{H}^3\beta^2)}{B^2q_2^2r_\mathrm{H}^2 + (B^2 + \beta^2 r_\mathrm{H}^3)^2}.\end{aligned} \tag{A11}$$

In general, we have the relation

$$\begin{pmatrix} J_i \\ Q_i \end{pmatrix} = \begin{pmatrix} \sigma_{ij} & \alpha_{ij}T \\ \bar{\alpha}_{ij}T & \bar{\kappa}_{ij}T \end{pmatrix}\begin{pmatrix} E_j \\ -(\nabla_j T)/T \end{pmatrix}. \tag{A12}$$

After obtaining the expressions for σ_{ij}, α_{ij}, and $\bar{\alpha}_{ij}$, the thermal conductivity can be read off from (A12). Considering the conditions $Q_x = 0, \nabla_y T = 0$, and $E_y = 0$, the thermal conductivity matrix component $\bar{\kappa}_{xx}$ is given by

$$\bar{\kappa}_{xx} = \frac{T\alpha_{xx}^2}{\sigma_{xx} - \sigma_{xx}^0}, \tag{A13}$$

where $\sigma_{xx}^0 = \sigma_{xx}(q_2 = 0)$ denotes the quantum critical conductivity. Similarly, the case $Q_x = 0, \nabla_x T = 0$, and $E_y = 0$ gives

$$\bar{\kappa}_{xy} = \frac{T\alpha_{xx}\alpha_{xy}}{\sigma_{xx}}. \tag{A14}$$

Therefore, we finally obtain

$$\bar{\kappa}_{xx} = \frac{16\pi^2 Tr_\mathrm{H}^3(B^2 + \beta^2 r_\mathrm{H}^3)}{B^2q_2^2r_\mathrm{H}^2 + (B^2 + \beta^2 r_\mathrm{H}^3)^2}, \tag{A15}$$

$$\bar{\kappa}_{xy} = \frac{16\pi^2 TBq_2 r_\mathrm{H}^4}{B^2q_2^2r_\mathrm{H}^2 + (B^2 + \beta^2 r_\mathrm{H}^3)^2}. \tag{A16}$$

These results are consistent with the results obtained in [13,14].

[1] *Handbook of High Temperature Superconductivity*, edited by J. R. Schrieffer (Springer Press, New York, 2007).

[2] S. Sachdev, *Quantum Phase Transitions* (Cambridge University Press, Cambridge, England, 1999).

[3] K. Damle and S. Sachdev, Nonzero-temperature transport near quantum critical points, Phys. Rev. B **56**, 8714 (1997).

[4] S. Sachdev and M. Mueller, Quantum criticality and black holes, J. Phys. Condens. Matter **21**, 164216 (2009).

[5] P. Phillips and C. Chamon, Breakdown of One Parameter Scaling in Quantum Critical Scenarios for the High-Temperature Copper-Oxide Superconductors, Phys. Rev. Lett. **95**, 107002 (2005).

[6] D. van der Marel, H. J. A. Molegraaf, J. Zaanen, Z. Nussinov, F. Carbone, A. Damascelli, H. Eisaki, M. Greven, P. H. Kes, and M. Li, Powerlaw optical conductivity with a constant phase angle in high T_c superconductors, Nature (London) **425**, 271 (2003).

[7] B. Keimer, S. A. Kivelson, M. R. Norman, S. Uchida, and J. Zaanen, High temperature superconductivity in the cuprates, Nature (London) **518**, 179 (2015).

[8] M. Blake and A. Donos, Quantum Critical Transport and the Hall Angle, Phys. Rev. Lett. **114**, 021601 (2015).

[9] Z. Zhou, J. P. Wu, and Y. Ling, Note on DC and Hall conductivity in holographic massive Einstein-Maxwell-Dilaton gravity, J. High Energy Phys. 08 (2015) 067.

[10] S. A. Hartnoll, Lectures on holographic methods for condensed matter physics, Classical Quantum Gravity **26**, 224002 (2009).

[11] J. McGreevy, Holographic duality with a view toward many-body physics, Adv. High Energy Phys. **2010**, 723105 (2010).

[12] C. P. Herzog, Lectures on holographic superfluidity and superconductivity, J. Phys. A **42**, 343001 (2009).

[13] A. Donos and J. P. Gauntlett, Thermoelectric DC conductivities from black hole horizons, J. High Energy Phys. 11 (2014) 081.

[14] M. Blake, A. Donos, and N. Lohitsiri, Magnetothermoelectric response from holography, J. High Energy Phys. 08 (2015) 124.

[15] K. Y. Kim, K. K. Kim, Y. Seo, and S. J. Sin, Thermoelectric conductivities at finite magnetic field and the Nernst effect, J. High Energy Phys. 07 (2015) 027.

[16] A. Amoretti and D. Musso, Universal formulae for thermoelectric transport with magnetic field and disorder, J. High Energy Phys. 09 (2015) 094.

[17] A. Amoretti, M. Baggioli, N. Magnoli, and D. Musso, Chasing the cuprates with dilatonic dyons, J. High Energy Phys. 06 (2016) 113.

[18] P. W. Anderson, *The Theory of Superconductivity in the High-T_c Cuprates* (Princeton University Press, Princeton, 1997).

[19] M. Ogata and P. W. Anderson, Transport Properties in the Tomonaga-Luttinger Liquid, Phys. Rev. Lett. **70**, 3087 (1993).

[20] A. Donos and J. P. Gauntlett, Holographic Q-lattices, J. High Energy Phys. 04 (2014) 040.

[21] Y. Ling, C. Niu, J. P. Wu, Z. Y. Xian, and H. Zhang, Metal-Insulator Transition by Holographic Charge Density Waves, Phys. Rev. Lett. **113**, 091602 (2014).

[22] T. Andrade and B. Withers, A simple holographic model of momentum relaxation, J. High Energy Phys. 05 (2014) 101.

[23] K. Y. Kim, K. K. Kim, Y. Seo, and S. J. Sin, Coherent/incoherent metal transition in a holographic model, J. High Energy Phys. 12 (2014) 170.

[24] B. Gouteraux, Charge transport in holography with momentum dissipation, J. High Energy Phys. 04 (2014) 181.

[25] R. A. Davison and B. Gouteraux, Momentum dissipation and effective theories of coherent and incoherent transport, J. High Energy Phys. 01 (2015) 039.

[26] X. H. Ge, Y. Ling, C. Niu, and S. J. Sin, Thermoelectric conductivities, shear viscosity, and stability in an anisotropic linear axion model, Phys. Rev. D **92**, 106005 (2015).

[27] A. Amoretti, A. Braggio, N. Maggiore, N. Magnoli, and D. Musso, Thermo-electric transport in gauge/gravity models with momentum dissipation, J. High Energy Phys. 09 (2014) 160.

[28] A. Amoretti, A. Braggio, N. Maggiore, N. Magnoli, and D. Musso, Analytic dc thermo-electric conductivities in holography with massive gravitons, Phys. Rev. D **91**, 025002 (2015).

[29] A. Donos and J. P. Gauntlett, Navier-Stokes equations on black hole horizons and dc thermoelectric conductivity, Phys. Rev. D **92**, 121901 (2015).

[30] E. Banks, A. Donos, and J. P. Gauntlett, Thermoelectric DC conductivities and Stokes flows on black hole horizons, J. High Energy Phys. 10 (2015) 103.

[31] A. Donos, J. P. Gauntlett, T. Griffin, and L. Melgar, DC conductivity of magnetised holographic matter, J. High Energy Phys. 01 (2016) 113.

[32] R. A. Davison and B. Gouteraux, Dissecting holographic conductivities, J. High Energy Phys. 09 (2015) 090.

[33] R. A. Davison, B. Gouteraux, and S. Hartnoll, Incoherent transport in clean quantum critical metals, J. High Energy Phys. 10 (2015) 112.

[34] S. Grozdanov, A. Lucas, S. Sachdev, and K. Schalm, Absence of Disorder-Driven Metal-Insulator Transitions in Simple Holographic Models, Phys. Rev. Lett. **115**, 221601 (2015).

[35] X. H. Ge, S. J. Sin, and S. F. Wu, Universality of DC electrical conductivity from holography, Phys. Lett. B **767**, 63 (2017).

[36] S. A. Hartnoll and A. Karch, Scaling theory of the cuprate strange metal, Phys. Rev. B **91**, 155126 (2015).

[37] A. Karch, Conductivities for hyperscaling violating geometries, J. High Energy Phys. 06 (2014) 140.

[38] D. V. Khveshchenko, Viable phenomenologies of the normal state of cuprates, Europhys. Lett. **111**, 17003 (2015).

[39] A. Karch, K. Limtragool, and P. W. Phillips, Unparticles and anomalous dimensions in the cuprates, J. High Energy Phys. 03 (2016) 175.

[40] X. Dong, S. Harrison, S. Kachru, G. Torroba, and H. Wang, Aspects of holography for theories with hyperscaling violation, J. High Energy Phys. 06 (2012) 041.

[41] M. Alishahiha, E. O. Colgain, and H. Yavartanoo, Charged black branes with hyperscaling violating factor, J. High Energy Phys. 11 (2012) 137.

[42] Z. Y. Fan and H. Lü, Electrically-charged Lifshitz spacetimes and hyperscaling violations, J. High Energy Phys. 04 (2015) 139.

[43] C. Martinez, C. Teitelboim, and J. Zanelli, Charged rotating black hole in three spacetime dimensions, Phys. Rev. D **61**, 104013 (2000).

[44] D. Maity, S. Sarkar, B. Sathiapalan, R. Shankar, and N. Sircar, Properties of CFTs dual to charged BTZ black-hole, Nucl. Phys. **B839**, 526 (2010).

[45] P. Chaturvedi and G. Sengupta, Conductivity oscillations, rotating BTZ black holes and holographic superconductors, Phys. Rev. D **90**, 046002 (2014).

[46] M. Cadoni and M. R. Setare, Near-horizon limit of the charged BTZ black hole and AdS_2 quantum gravity, J. High Energy Phys. 07 (2008) 131.

[47] J. W. Loram, K. A. Mirza, J. M. Wade, J. R. Cooper, and W. Y. Liang, The electronic specific heat of cuprate superconductors, Physica C: Superconductivity **235**, 134 (1994).

[48] A. Donos, J. P. Gauntlett, J. Sonner, and B. Withers, Competing orders in M-theory: superfluids, stripes and metamagnetism, J. High Energy Phys. 03 (2013) 108.

[49] T. Faulkner, H. Liu, and M. Rangamani, Integrating out geometry: Holographic Wilsonian RG and the membrane paradigm, J. High Energy Phys. 08 (2011) 051.

[50] I. Heemskerk and J. Polchinski, Holographic and Wilsonian renormalization groups, J. High Energy Phys. 06 (2011) 031.

[51] S. J. Sin and Y. Zhou, Holographic Wilsonian RG flow and sliding membrane paradigm, J. High Energy Phys. 05 (2011) 030.

[52] X. H. Ge, Y. Ling, Y. Tian, and X. N. Wu, Holographic RG flows and transport coefficients in Einstein-Gauss-Bonnet Maxwell theory, J. High Energy Phys. 01 (2012) 117.

[53] I. Bredberg, C. Keeler, V. Lysov, and A. Strominger, Wilsonian approach to fluid/gravity duality, J. High Energy Phys. 03 (2011) 141.

[54] Y. Tian, X. H. Ge, and S. F. Wu, Wilsonian RG approach to transport with momentum dissipation, arXiv:1702.05470 [Phys. Rev. D (to be published)].

[55] Y. Zhang, N. Ong, Z. Xu, K. Krishana, R. Gagnon, and L. Taillefer, Determining the Wiedemann-Franz Ratio from the Thermal Hall Conductivity: Application to Cu and $YBa_2Cu_3O_{6.95}$, Phys. Rev. Lett. **84**, 2219 (2000).

[56] Y. Wang, L. Li, and N. P. Ong, Nernst effect in high-T_c superconductors, Phys. Rev. B **73**, 024510 (2006).

[57] M. Matusiak, S. H. Naqib, I. Kokanovic, and J. R. Cooper, Influence of the pseudogap on the Nerst coefficient of $Y_{0.9}Ca_{0.1}Ba_2\ Cu_3O_y$, Europhys. Lett. **86**, 17005 (2009).

[58] In conventional metals, the Nernst signal is linear in the magnetic field.

[59] J. S. Kim, B. H. Kim, D. C. Kim, and Y. W. Park, Thermoelectric power of $La_{2-x}Sr_xCuO_4$ at high temperature, Ann. Phys. (Leipzig) **13**, 43 (2004).

[60] J. Crossno *et al.*, Observation of the Dirac fluid and the breakdown of the Wiedemann-Franz law in graphene, Science **351**, 1058 (2016).

[61] S. A. Hartnoll, P. K. Kovtun, M. Mueller, and S. Sachdev, Theory of the Nernst effect near quantum phase transitions in condensed matter, and in dyonic black holes, Phys. Rev. B **76**, 144502 (2007).

[62] H. Pfau *et al.*, Thermal and electrical transport across a magnetic quantum critical point, Nature (London) **484**, 493 (2012).

[63] T. Senthil, M. Vojta, and S. Sachdev, Weak magnetism and non-Fermi liquids near heavy-fermion critical points, Phys. Rev. B **69**, 035111 (2004).